Synthesis of Star–Comb-Shaped Polymer with Porphyrin-Core and its Self-Assembly Behavior Study

Bao Zhang,[1,2] Di Wang,[3] Meng Li,[1] Yapeng Li,[1,2] Xuesi Chen[2]

[1]*Alan G. MacDiarmid Institute, College of Chemistry, Jilin University, Changchun 130012, China*
[2]*Key Laboratory of Polymer Ecomaterials, Changchun Institute of Applied Chemistry, Chinese Academy of Sciences, Changchun 130022, China*
[3]*Department of Chemistry, Changchun Normal University, Changchun 130032, China*

Received 26 July 2011; accepted 18 January 2012
DOI 10.1002/app.36835
Published online in Wiley Online Library (wileyonlinelibrary.com).

ABSTRACT: 5,10,15,20-tetra(4-hydroxyphenyl)porphyrin (THPP) was synthesized by the condensation of pyrrole with 4-hydroxybenzaldehyde in the presence of solvent (propionic acid). Subsequently, the resulting THPP was converted to a tetrafunctional star-shaped macroinitiator (porphyrin-Br_4) by esterification of it with 2-bromopropanoyl bromide, and then atom transfer radical polymerization (ATRP) of styrene was conducted at 110°C with CuCl/2,2′-bipyridine as the catalyst system. The resulting product was reacted with NBS to obtain star-shaped initiator porphyrin-(PSt-$Br)_4$, which was used the following ATRP of the GMA to synthesize star–comb-shaped grafted polymer porphyrin-(PSt-*g*-$PGMA)_4$. The number molecular weight was 2.3×10^4 g/mol, and the dispersity was narrow ($M_w/M_n = 1.32$). The structure of the polymers was investigated by NMR, UV–vis, IR, and GPC measurement. The self-assembly behavior of the polymer porphyrin-(PSt-*g*-$PGMA)_4$ was studied by DLS and AFM. © 2012 Wiley Periodicals, Inc. J Appl Polym Sci 000: 000–000, 2012

Key words: atom transfer radical polymerization (ATRP); block copolymers; self-assembly; star polymers

INTRODUCTION

Porphyrins are a group of organic compounds with macrocycle conjugated structure, which have received considerable attention due to their interesting excited state chemical properties, electron-transfer processes, biological processes, photo-physical and catalytic properties.[1–3] However, low solubility of porphyrins in common organic solvents and their easy aggregation are stumbling blocks towards their potential technological applications. To make an intensive study of the application of porphyrin, it is necessary to synthesize porphyrin with active functional groups. Among of them, functionalized 5,10,15,20-tetrasubstituted porphyrin is a most promising one, whose substituents contain chemically reactive groups such as halogens, alcohols, esters, or pseudohalogens, would present suitable precursors for the synthesis of more complicated porphyrin systems with special physical and chemical properties or those that could be easily transformed into amphiphilic porphyrins.[4–9]

Correspondence to: Y. Li (liyapeng@jlu.edu.cn) or X. Chen (xschen@ciac.jl.cn).

Contract grant sponsor: National Natural Science Foundation of China; contract grant number: 20574028.

Star-shaped polymers have been received great interest since Schaefgen and Flory first proposed this concept in 1948[10] because of their unique properties such as impact-resistant plastics, different phase behavior, thermoplastic elastomers, variety of morphologies, polymeric emulsifiers, sol–gel states, and gas permeation membranes.[11–13] As another type of polymers with unique construction, comb-shaped polymers have been studied widely, which are types of macromolecules with densely grafted side chains on a linear backbone.[14,15] Because of the crowded side chains on the backbone, the main chain of a molecular brush is extended, and as a result the molecule tends to make spherical, cylindrical, or worm-like configurations.[16–18] As a type of more structurally complex polymer, star–comb-shaped copolymers were reported rarely due to the difficulty in synthesis.[19] But their unique performances were very attractive. Therefore, it is a promising work to explore new method for the synthesis of star–comb-shaped copolymers.

In the past decade, the synthesis of star-shaped porphyrin-centered polymers have attracted great interest.[20–26] In particular, recent advances in controlled radical polymerization techniques yield well-defined star-shaped porphyrin-centered polymers. These polymers have been prepared via nitroxide radical-mediated radical polymerization,[27] reversible addition-fragmentation chain transfer (RAFT) radical

TABLE I
Experimental Conditions and Results for the Synthesis of Porphyrin-(PSt)$_4$, Porphyrin-(PSt-Br)$_4$, and Porphyrin-(PSt-*g*-PGMA)$_4$ Polymers

Sample	$[M]_0/[I]_0$	Time (h)	Monomer[a] conversion	M_n(th)[b] (g/mol)	M_n(NMR)[a] (g/mol)	M_n(GPC)[c] (g/mol)	M_w/M_n[c]
Porphyrin-(PSt)$_4$	200/1	10	38.20%	8.7×10^3	9.2×10^3	8.9×10^3	1.28
Porphyrin-(PSt-Br)$_4$						9.8×10^3	1.30
Porphyrin-(PSt-*g*-PGMA)$_4$	200/1	4	50.20%	1.6×10^4	1.8×10^4	$2.3 \times 1\ 0^4$	1.32

[a] Determined by ^{1}H-NMR analysis.
[b] The theoretical molecular weights ($M_{n.\mathrm{th}}$) calculated from the ratio of the monomer to the initiator $[M]_0/[I]_0$ and the monomer conversion. $M_{n.\mathrm{th}} = ([M]_0/[I]_0) \times M_{\mathrm{monomer}} \times \mathrm{con.\%} + M_{n,\mathrm{initiator}}$.
[c] Determined by GPC measurements.

polymerization,[28,29] and atom transfer radical polymerization (ATRP) methods.[30,31] Especially, ATRP[32] has provided a powerful tool for the preparation of well-defined polymers and for macromolecular design due to the suitability of most (meth)acrylate and styrenic monomers and their compatibility with a wide range of solvents. Most importantly, the tolerance of functional groups and impurities makes ATRP a versatile technique for the preparation of complex polymer molecules with special functionalities.

In this work, we concentrated on the synthesis of star-comb shaped copolymer porphyrin-(PSt-*g*-PGMA)$_4$ with porphyrin-core by the ATRP reaction. To the best of our knowledge, star-comb shaped polymers with porphyrin-core have not been reported so far. The novel star–comb copolymers have the advantages of porphyrin, star polymers and comb polymers, which make them promising in physical, chemical, and biological application. The current study proposed a feasible method for the synthesis star–comb copolymers. The structure and composition of polymers were characterized with UV–vis, NMR, GPC, and FTIR. Some results are given in Table I. Amphiphilic star–comb-shaped polymer porphyrin-(PSt-*g*-PGMA)$_4$ based on porphyrin units, PSt and epoxy-functional moieties is attractive to prepare polymeric materials potentially useful in advanced biotechnology. In addition, the self-assembly behavior of porphyrin-(PSt-*g*-PGMA)$_4$ star–comb-shaped polymer was also studied in aqueous media.

EXPERIMENTAL

Materials

Glycidyl methacrylates (GMA) were obtained from Aldrich Chemical and distilled with calcium hydride (CaH_2) under vacuum before use. *N*-bromosuccinimide (NBS) (Aldrich, 99%), α-bromopropanoyl bromide (Aldrich, 99%), 4-hydroxybenzaldehyde (Alfa Aesar, 98%), and propionic acid (Tianjin Tiantai) were used without further purification. Pyrrole (Shanghai Kefeng) was distilled before use. Styrene (Beijing Chemical) was distilled over CaH_2 in vacuum before use. Copper(I) chloride (CuCl, Beijing Chemical) was purified by precipitation from acetic acid to remove Cu^{2+}, filtrated and washed with ethanol and then dried. 2, 2′-Bipyridine (bpy, Beijing Chemical), tetrahydrofuran (Beijing Chemical), and dichloromethane (Tianjin Chemical) were dried with CaH_2 and distilled. *N*,*N*′-dimethylformamide (DMF) was dried with CaH_2 and distilled under vacuum before use. Triethylamine (TEA, Beijing Chemical) was refluxed for 12 h in the presence of CaH_2 and distilled. All the reagents used in this study were of analytic grade.

Synthesis of THPP

Propionic acid (60 mL), acetic acid (60 mL), and nitrobenzene (60 mL) were added to a three-necked round-bottomed flask in an oil bath with constant temperature that the mixed solvents were refluxed. 4-Hydroxybenzaldehyde (7.33 g, 60 mmol) in 40 mL propionic acid and the pyrrole (4.16 mL, 60 mmol) in 40 mL nitrobenzene were added dropwise to the flask using two dropping funnels with stirring over a period of 30 min. And then the reaction was carried out for 40 min. After the mixture was cooled, the black solid matters was separated out via filtration and evaporated in vacuum. The crude product was purified with column chromatography and the pure THPP (1 of Scheme 1) was obtained. ^{1}H-NMR (DMSO-d_6, δ): 9.96 (s, 4H, —OH), 8.87 (d, 8H, pyrrole ring), 8.00 (d, 8H, benzene ring), 7.21 (d, 8H, ArH), −2.88 (s, 2H, pyrrole NH).

Synthesis of the star-initiator porphyrin-(Br)$_4$

THPP (0.5 g, 0.625 mmol) dissolved in 15 mL THF was mixed with pyridine (0.99 g, 12.5 mmol) and α-bromopropanoyl bromide (2.7 g, 12.5 mmol) in a 100-mL round-bottomed flask. The reaction was carried out at room temperature for 24 h under stirring continuously. The solution was passed through a neutral alumina chromatography column to remove the quaternary ammonium halide $(CH_3CH_2)_3NH^+Cl^-$.

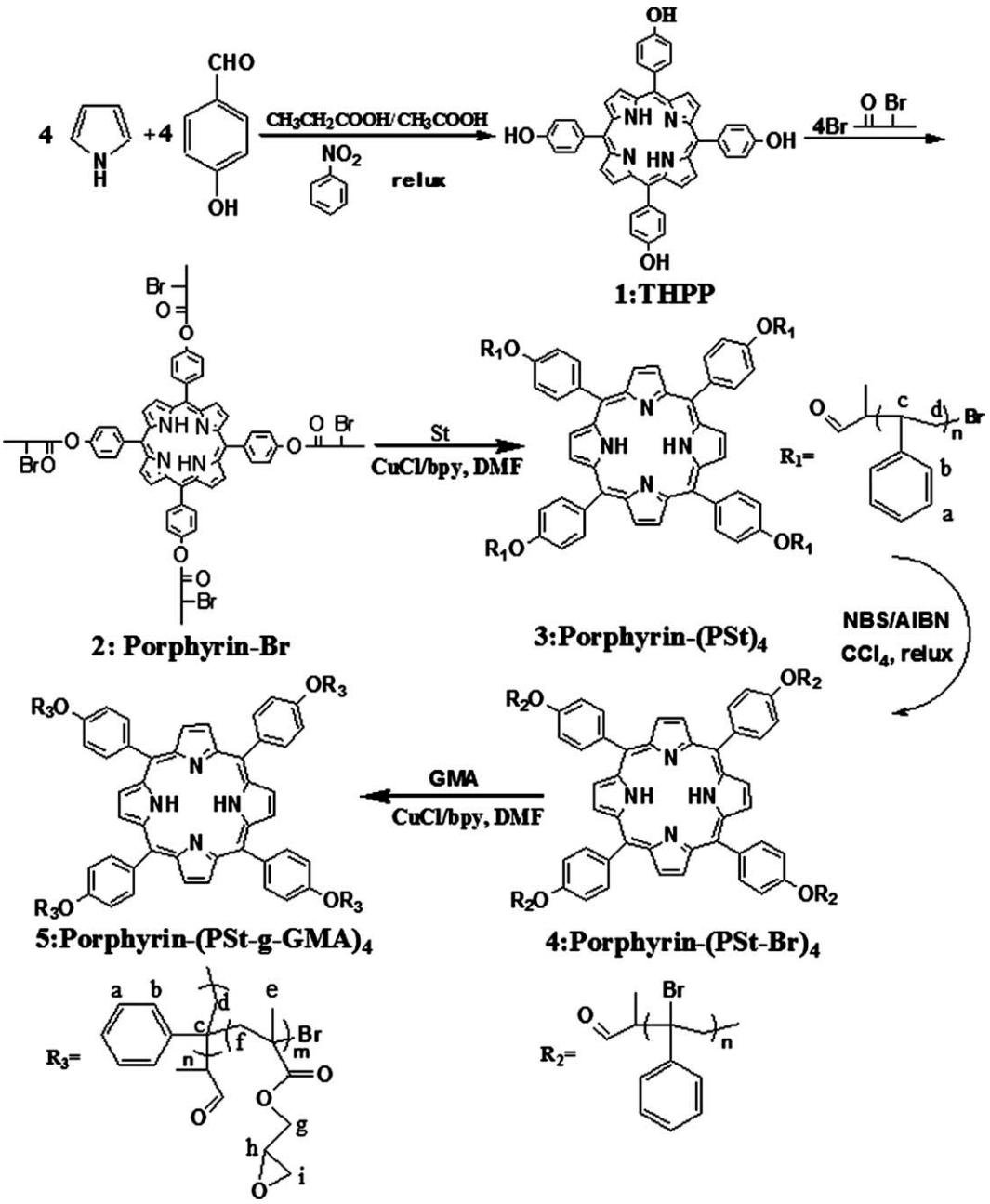

Scheme 1 The synthesis of porphyrin-(PSt-*g*-PGMA)$_4$.

The filtrate was removed by rotary evaporation and the pure product, porphyrin-(Br)$_4$ (2 in Scheme 1), was obtained. ^{1}H-NMR ($CDCl_3$, δ): 8.88 (d, 8H, pyrrole ring), 8.24 (d, 8H, benzene ring), 7.56 (d, 8H, benzene ring), 4.36 (m, 1H, >CH—), −2.85 (s, 2H, pyrrole NH), 1.80 (d, 3H, —CH_3).

Synthesis of the star polymer porphyrin-(PSt)$_4$

A dry flask equipped with a magnetic stirrer was charged with CuCl (0.018 g, 1.89×10^{-4} mol), bpy (0.084 g, 5.49×10^{-4} mol), and multi-functional star-initiator (0.135 g, 1.0×10^{-4} mol). The reaction vial was sealed and degassed three times by freeze-pump–thaw cycles. Solvent THF (1.0 mL) and monomer styrene (2.08 g, 0.02 mol) degassed by inert dry argon were introduced into the flask via an Ar-washed syringe. After initiator was completely dissolved, the reaction flask was placed into a constant temperature (110°C) oil bath with magnetic stirring for a predetermined time. The reaction was rapidly terminated in an ice bath. The catalyst was removed by passage of the polymer solution through an aluminum oxide column. The crude polymer was precipitated in methanol, and then dried under vacuum overnight. ^{1}H-NMR ($CDCl_3$, δ):

8.88 (d, 8H, pyrrole ring), 8.24 (d, 8H, benzene ring in porphyrin), 7.56 (d, 8H, benzene ring in porphyrin), 6.3–7.0 (m, aromatic protons), 0.90–2.18 (m, CH and CH_2 in PSt).

Removal of bromide end groups to obtain halogen-free porphyrin-$(PSt)_4$

Porphyrin-$(PSt)_4$ (M_n = 9200 g/mol and M_w/M_n = 1.28; 0.736 g, 8 × 10^{-5} mol) was dissolved in a mixture of triethylamine (3 mL) and CH_2Cl_2 (3 mL) in a 50-mL flask and purged with argon for 1 h. CuCl (0.016 g, 1.6 × 10^{-4} mol) and HMTETA (0.37 g, 1.6 × 10^{-3} mol mmol) were added to this stirred solution under argon. The mixture was stirred at 50°C under argon for 3 days. The resulting reaction mixture was exposed to air and diluted with CH_2Cl_2, followed by passing through a silica column to remove the residual catalyst. After rotary evaporation to remove most of the CH_2Cl_2 and triethylamine, the crude halogen-free polymer porphyrin-$(PSt)_4$ was precipitated into excess methanol and dried in vacuum. The yield was 80%.

Confirmation of removal of bromine end groups

The efficiency of the removal of the bromine end groups was assessed by ATRP of styrene with the halogen-free porphyrin-$(PSt)_4$ as a macroinitiator. No chain extension occurred if the terminal Br atoms were absent. A typical process was as follows. CuCl (0.003 g, 3 × 10^{-5} mol), bpy (0.0148 g, 9 × 10^{-5} mol), and porphyrin-$(PSt)_4$ (0.092 g, 1 × 10^{-5} mol) were added into a flask equipped with a magnetic stirrer. The reaction flask was sealed with a rubber septum and immersed in an ice water/NaCl mixture at about −10°C and followed by three cycles of vacuum-argon to remove the oxygen. Solvents toluene (1 mL) and monomer styrene (1.08 g, 0.01 mol) degassed by argon were introduced into the flask via an Ar-washed syringe. After the macroinitiator was dissolved completely, the flask was placed into an oil bath at 120°C. After stirring for 10 h, the reaction mixture was exposed to air. The resulting polymer was characterized by GPC measurement.

Bromination of porphyrin-$(PSt)_4$

The bromination of porphyrin-$(PSt)_4$was carried out according to the report described previously.[33,34] NBS (0.342 g), AIBN (0.052 g), porphyrin-$(PSt)_4$ (1.5 g), and CCl_4 (60 mL) were added into a flask equipped with a magnetic stirrer. After refluxing at 90°C for 5 h, the reaction mixture was filtered. The filtrate was concentrated and precipitated in methanol, dried in a vacuum oven overnight.

Synthesis of the star–comb-shaped polymer porphyrin-(PSt-*g*-PGMA)$_4$

A dry flask equipped with a magnetic stirrer was charged with CuCl (0.018 g, 1.8 × 10^{-4} mol), bpy (0.084 g, 5.4 × 10^{-4} mol), and initiator star-initiator porphyrin-$(PSt\text{-}Br)_4$ (0.24 g, 2.60 × 10^{-5} mol). The reaction vial was sealed and degassed three times by freeze-pump–thaw cycles. Pre-degassed solvent DMF (1.0 mL) and monomer GMA (0.52 g, 5.2 × 10^{-3} mol) by argon were introduced into the flask via an Ar-washed syringe. Subsequently, the reaction flask was immersed in a constant temperature (80°C) oil bath for the given time. The reaction was rapidly terminated in an ice bath. The catalyst was removed by passage of the polymer solution through an aluminum oxide column. The crude polymer was precipitated in methanol, and then dried under vacuum overnight.

Sample preparation

The silicon wafers were cleaned in a piranha solution (70/30 v/v of concentrated H_2SO_4 and 30% H_2O_2) at 90°C overnight, thoroughly rinsed with deionized water, and finally blown dry with nitrogen. The preparation of nanospheres was done as follows. First, porphyrin-(PSt-*g*-PGMA)$_4$ was dissolved in distilled THF at room temperature to obtain molecularly dispersed and homogeneous solution. The blue tint solution appeared when distilled water (50 mL) was added dropwise into the copolymer solution with stirring, indicating the formation of nanospheres. After the mixture was sonicated for about 1 h at room temperature, the solution was analyzed by DLS. About 1 mL of the nanosphere solvent was dropped onto the silicon wafer surface. The silicon wafer covered with nanospheres was dried in a desiccator, and then analyzed by means of AFM.

Characterization

^1H and ^{13}C nuclear magnetic resonance (NMR) spectra were recorded on a Bruker ARX-500 NMR spectrometer with $CDCl_3$ or dimethyl sulfoxide (DMSO-d_6) as solvent at 500 and 125 MHz, respectively. Chemical shifts (ppm) were referenced on the δ scale downfield from the trimethylsilane (TMS) signal as internal standard. The molecular weights and molecular weight distributions were measured on a Waters 410 gel permeation chromatography (GPC) apparatus equipped with a 10-μm Styragel HT6E column (300 mm × 7.8 mm) with linear polystyrene standards. THF was used as the eluant at a flow rate of 1 mL/min. The infrared spectra (IR) of polymers were recorded on a Nicolet Impact 410 at room temperature. Dried samples (20 mg) were

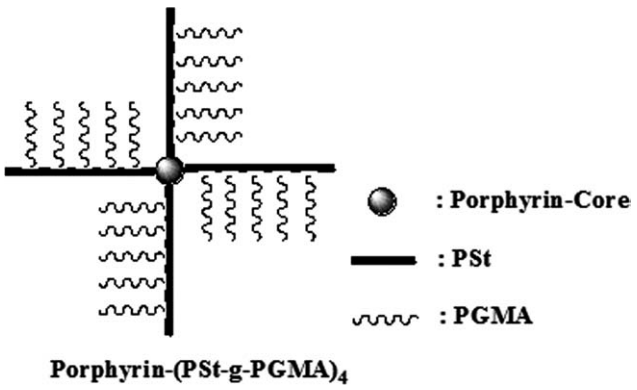

Figure 1 The sketch of the star–comb polymer.

mixed with 100 mg of dry KBr and pressed into disk (100 kg/cm^2). UV/vis spectra were collected using Varian Cary 5000 UV-VIS-NIR spectrometer and using DMF as solvent. The atomic force microscopy (AFM) observations of the morphologies absorbed on a freshly treated silicon wafer surface were carried out with the commercial instrument (Digital Instrument, Nanoscope IIIa, Multimode). All the tapping mode images were taken at room temperature in air with the microfabricated rectangle crystal silicon cantilevers (nanosensor). The topography images were obtained at a resonance frequency of approximate 365 kHz for the probe oscillation. Dynamic light scattering (DLS) (Brookhaven BI9000AT) studies were carried out using a goniometer equipped with He-Ne laser at scattering angle of 90°.

RESULTS AND DISCUSSION

Synthesis of THPP

The synthesis of THPP (Fig. 1) has been investigated widely. Generally, the synthesis was carried out by two steps method, and the yield was low. In this work, it was proved that the THPP synthesized by the condensation of pyrrole with 4-hydroxybenzaldehyde in the presence of mixed solvents was very effective, and the product yield could be increased from 20%[35] to 39%. The synthesis of the star–comb-shaped polymer porphyrin-(PSt-*g*-PGMA)$_4$ was depicted in Scheme 1.

The structure of the THPP was determined by ^{1}H-NMR spectrum [Fig. 2(A)], in which the single signal **a** at −2.88 ppm represented the porphyrin macrocycle protons of the center, the single signal **e** at 9.96 ppm corresponded to the hydroxyl protons of porphyrins cycle. Also, the single signal **d** at 8.87 ppm attributed to the pyrrole rings protons of porphyrins, the double signals **c, b** at 7.21 and 8.00 ppm belonged to the phenyl of porphyrins cyclic. The FTIR spectra of THPP are shown in Figure 3(A). The intensive absorption bands appeared in the wavenumber region of ~ 2936 cm^{-1}, 1490 cm^{-1}, and 674 cm^{-1} were ascribed to the ring vibration of the aromatic group of THPP. The peak at wavenumber of 3368 cm^{-1} was assigned to the absorption band of the amide N-H group of the THPP. Further evidence of THPP was gained by observing the absorption band at 1175 and 3436 cm^{-1} due to the vibration absorption of the C—O—H group of the

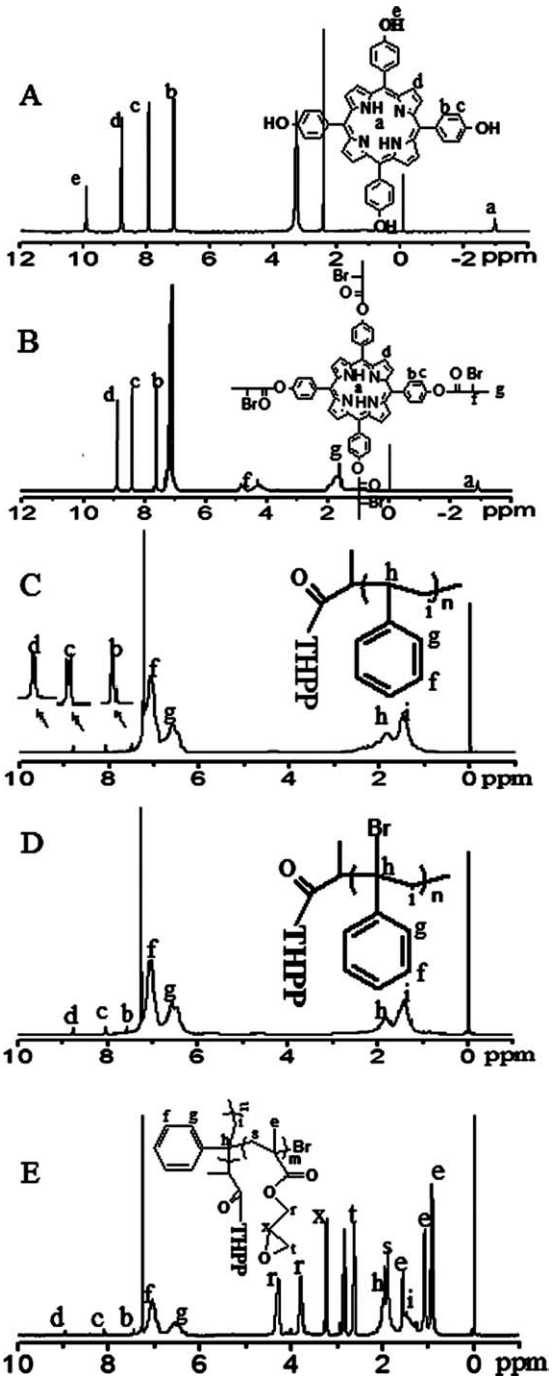

Figure 2 The ^{1}H-NMR spectrum of THPP 1 (A) was recorded at room temperature in DMSO; Porphyrin-Br 2 (B), porphyrin-(PSt)$_4$ 3 (C), porphyrin-(PSt-Br)$_4$ 4 (D), and porphyrin-(PSt-*g*-PGMA)$_4$ 5 (E) were recorded at room temperature in $CDCl_3$.

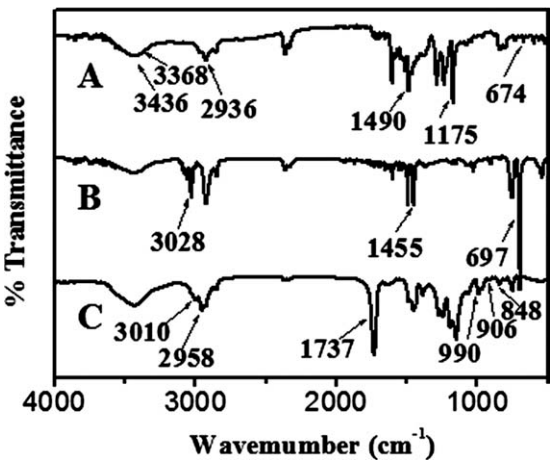

Figure 3 FTIR spectra of THPP (A), the star polymer porphyrin-$(PSt)_4$ (B), and porphyrin-$(PSt\text{-}g\text{-}PGMA)_4$ (C).

THPP. The ^{1}H-NMR analysis and IR results indicated the formation of the THPP.

Synthesis of the star-initiator porphyrin-$(Br)_4$

In the process, triethylamine was used as the catalyst to absorb HCl from the solution to generate a precipitate of quaternary ammonium halide $(CH_3CH_2)_3NH^+Cl^-$, which benefited the esterification. Compared with the ^{1}H-NMR spectrum of THPP, the OH signal of THPP at 9.96 ppm was disappeared completely after esterification. Moreover, the signals **f** and **g** at 4.36 ppm and 1.80 ppm assigned to the >CH— protons and the CH_3- protons closed to the active bromide, respectively, were also able to be detected [Fig. 2(B)], which indicated that the α-bromoester group was attached to the THPP end.

The spectral property of porphyrin and its ramification had attracted a lot attention of people. Figure 4(A) shows the UV/vis spectrum of THPP in DMF, and the insert was the 10 times amplified picture of the signals from 550 to 700 nm. The solution of THPP displayed spectra features that are commonly observed for porphyrins: an intense B (soret) band signals (418 nm) accompanied by four weaker signals Q band absorption at 516, 552, 594, and 661.5 nm. After the formation of porphyrin-Br_4, B (soret) band signals shows blue shift to 414.5 nm, and Q band shows blue shift to 512.5, 547, 589, and 646 nm. Because the introduction of carbonyl bromide group influenced the π-bond electron cloud density of porphyrin cycle.

Synthesis of the star polymer porphyrin-$(PSt)_4$

From the ^{1}H-NMR spectrum of the star-shaped polymer porphyrin-$(PSt)_4$ [Fig. 2(C)], it could be seen that besides the porphyrin signals **b–d**, the occurrence of the signals at 6.4–7.3 ppm corresponding to aromatic protons **f** and **g** of the PSt block proved the PSt

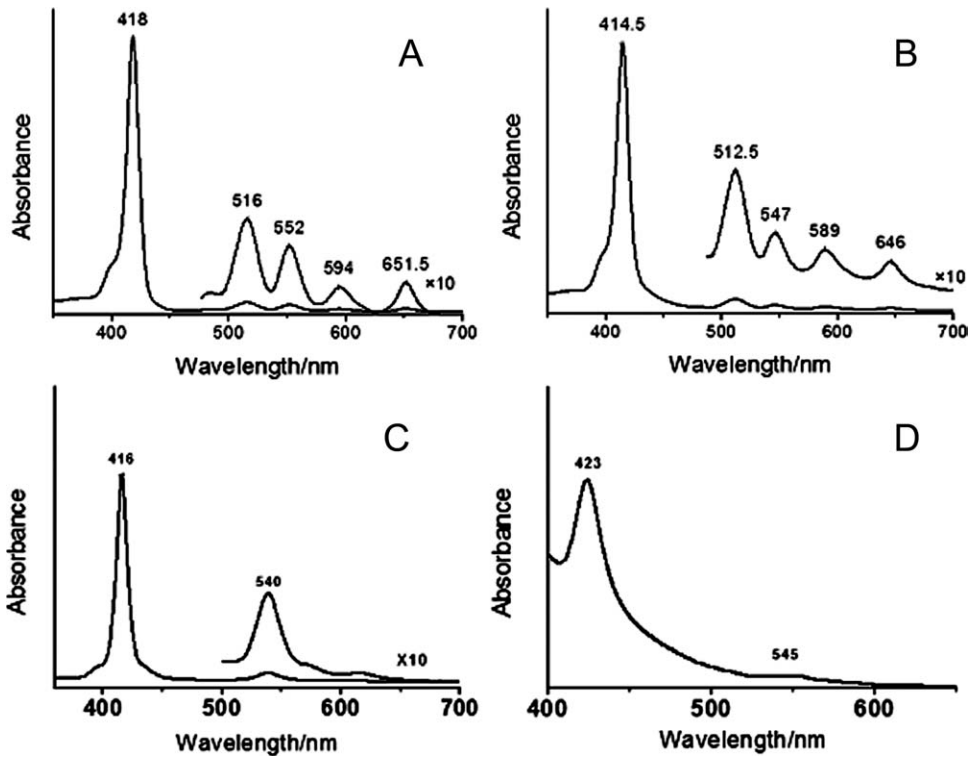

Figure 4 The UV/vis spectrum of THPP (A), porphyrin-Br_4 (B), porphyrin-$(PSt)_4$ (C), and porphyrin-$(PSt\text{-}g\text{-}PGMA)_4$ (D) were recorded at room temperature in DMF.

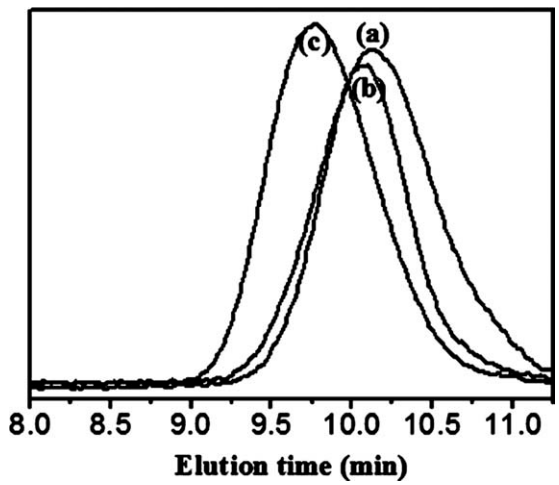

Figure 5 GPC plots of the porphyrin-$(PSt)_4$ (a), the initiator porphyrin-$(PSt\text{-}Br)_4$ (b), and star–comb copolymer porphyrin-(PSt-*g*-$PGMA)_4$ (c).

segments were connected with porphyrin cycle. In the IR spectra of the porphyrin-$(PSt)_4$ [Fig. 3(B)], porphyrin-$(PSt)_4$ polymers showed new peaks at wavenumbers of about 3028 cm^{-1}, 1455 cm^{-1}, and 697 cm^{-1}, which were ascribed to the ring vibration of the aromatic group of PSt. In this reaction, part of Cu^{2+} was introduced into the porphyrin core in the process of ATRP, and porphyrin metal complex was formed. Comparing GPC analysis, it was clear that the dispersity was less than 1.50 (1.28). The results clarified that no significant influence was occurred, and the reaction was still well controlled.

Star polymer porphyrin-$(PSt)_4$ synthesized by ATRP of styrene leads to PSt chains with bromide terminal groups. To avoid its influence on the following polymerization, we removed the bromide terminal groups. The efficiency of the removal of bromine end groups was assessed by the ATRP of styrene monomer with the halogen-free porphyrin-$(PSt)_4$ as a macroinitiator. The reaction process was shown in experiment section. The GPC results showed that no chain extension was detected, indicating that the porphyrin-$(PSt)_4$ did not initiate the polymerization. This control experiment confirmed the efficient removal of the terminal Br atoms from the porphyrin-$(PSt)_4$ precursor. The results were in agreement with previous reports.[36,37]

Bromination of porphyrin-$(PSt)_4$

The brominated porphyrin-$(PSt)_4$ was used as an organic halide initiator in the presence of CuCl combined with the ligand bpy as the catalyst, to graft GMA. Figure 2(C,D) shows the ^{1}H-NMR spectra of starting porphyrin-$(PSt)_4$ and the brominated products. The resonances at 1.9 and 1.4 ppm are assigned to CH and CH_2 units in the porphyrin-$(PSt)_4$ backbone, respectively. After bromination, the intensity ratio of the CH_2 and CH resonances increased from 2 to 2.19 due to the decrease in peak intensity of the CH unit as a consequence of benzylic bromination. The bromine content of the resultant polymer, estimated from the above integration ratios (8.67 mol %) are similar to elemental analysis values (9.1 mol %). This difference could be the consistence of bromide terminal groups at the end of the star polymer porphyrin-$(PSt)_4$. This confirms that the benzylic carbon is the predominant site of bromination. Considering the structure of porphyrin-$(PSt)_4$, the distribution of bromine atoms along the polymer backbone should be uniform.

Synthesis of the star–comb-shaped polymer porphyrin-(PSt-*g*-$PGMA)_4$

For the porphyrin-$(PSt\text{-}Br)_4$ initiator, partial bromination of porphyrin-$(PSt)_4$ at the benzylic positions gives star polymer porphyrin-$(PSt)_4$ having both terminal and side bromide groups. The use of such a star polymer as an initiator will result in synthesis of grafting of GMA onto PSt chains (PSt-*g*-PGMA), together with a small quality of graft copolymerization of GMA with PSt chains (PSt-*b*-PGMA). From the ^{1}H-NMR spectra of the porphyrin-(PSt-*g*-$PGMA)_4$ [Fig. 2(E)], it can be seen that besides the dominant porphyrin-$(PSt\text{-}Br)_4$ signals, there are also the occurrence of signals at 4.30 ppm and 3.81 ppm due to the splitting of methylene protons in the —CH_2OCO— group of the GMA unit by the methyne proton of the epoxy group. The peaks at 3.21 ppm and at 2.63, 2.83 ppm are assigned to the methyne proton and methylene protons of the epoxy group, respectively. The absorption bands at 0.9–1.4 ppm ascribed to the methyl group in the PGMA. According to the IR spectrum showed in Figure 3(C), the occurrence of the new absorption bands at the wavenumbers of about 848 cm^{-1}, 906 cm^{-1}, and 990 cm^{-1} ascribed to the epoxy group. The characteristic bands at 2958 cm^{-1} and 3010 cm^{-1} were assigned to the stretching of methyl group in the α-position with regard to the ester group. The intensive absorption bands appeared in the wave number

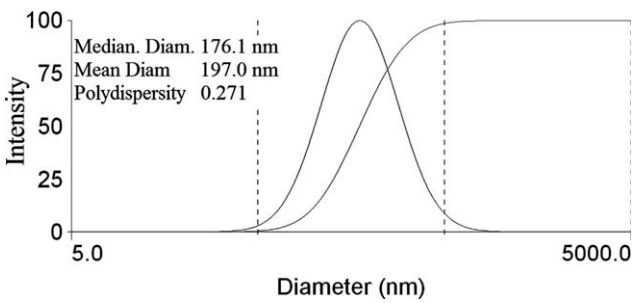

Figure 6 DLS result of porphyrin-(PSt-*g*-$PGMA)_4$.

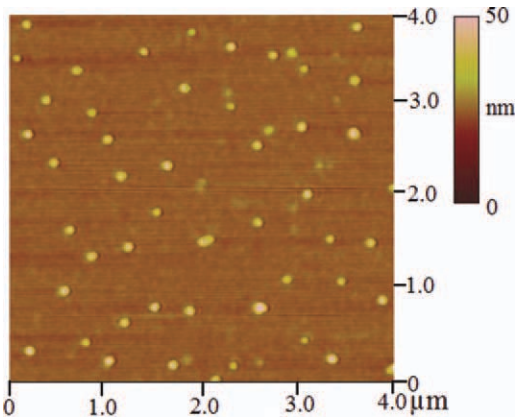

Figure 7 AFM image of porphyrin-(PSt-*g*-PGMA)$_4$. [Color figure can be viewed in the online issue, which is available at wileyonlinelibrary.com.]

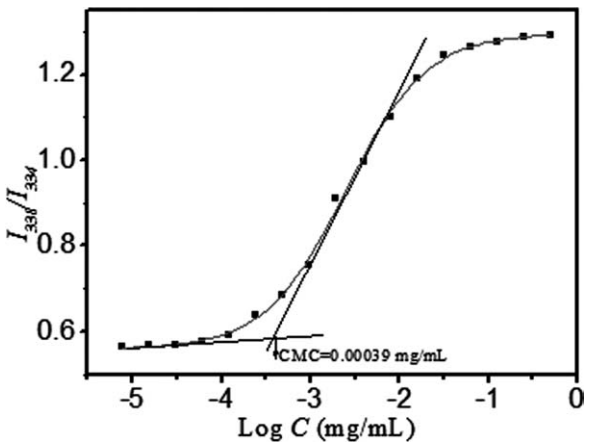

Figure 8 Plots of the fluorescence intensity ratios I_{338}/I_{334} from the excitation spectrum of pyrene probe as a function of polymer concentration C for porphyrin-(PSt-*g*-PGMA)$_4$.

region of 1737 cm^{-1} assigned to the ester carbonyl group of the PGMA main chains. The above result confirmed that the PGMA block was grafted onto the star-shaped initiator porphyrin-(PSt-Br)$_4$.

In contrast to the UV/vis spectrum of THPP, porphyrin-(Br)$_4$, porphyrin-(PSt)$_4$, and porphyrin-(PSt-*g*-PGMA)$_4$ show obvious change in the UV/vis spectra. For the porphyrin-(Br)$_4$ [Fig. 4(B)], the B (soret) band signals and Q band signals showed obvious blue shift (from 418 nm to 414 nm) due to the introduction of carbonyl bromide group influenced the π-bond electron cloud density of porphyrin cycle. For the porphyrin-(PSt)$_4$ [Fig. 4(C)], the B (soret) band signals showed obvious blue shift (from 418 to 416 nm), and Q band signals were reduced to one peak. It can be explained from two aspects. First, the porphyrins core and PSt arms of the star-shaped polymers were not in the same plane, which decreased the symmetry of molecular plane and influenced the degree of the conjugate of the π-bond in the porphyrin ring. Second, Cu^{2+} was introduced into the porphyrin core in the process of ATRP, and part of porphyrin metal complex was formed. The symmetry of porphyrin molecular was increased due to the Cu^{2+} enters into the porphyrin-core. The result of both factors was to decrease effective conjugate length of the porphyrin ring, so the spectroscopy showed blue shift. For the porphyrin-(PSt-*g*-PGMA)$_4$ [Fig. 4(D)], the B (soret) band signals showed obvious red shift (from 418 nm to 423 nm), and the Q band signals were also reduced to one peak. This also can be explained by above analysis. In addition, the introduction of PGMA chains further influenced molecular plane of star–comb copolymers. The result of above factors resulted in the increase of effective conjugate length of the porphyrin ring, so the spectroscopy showed red shift.

The evolution of the GPC curves is demonstrated in Figure 5. No obvious shoulders and tailings were observed in the GPC traces, and which suggested a high initiation efficiency and negligible radical–radical coupling in the polymerization. The unimodal and symmetrical shape on the GPC plot of the block copolymer suggested the complete initiation of the initiator during the ATRP process.

Self-assembly of star–comb polymer porphyrin-(PSt-*g*-PGMA)$_4$

The well-defined star–comb copolymer porphyrin-(PSt-*g*-PGMA)$_4$ consisting of a soft PGMA block and

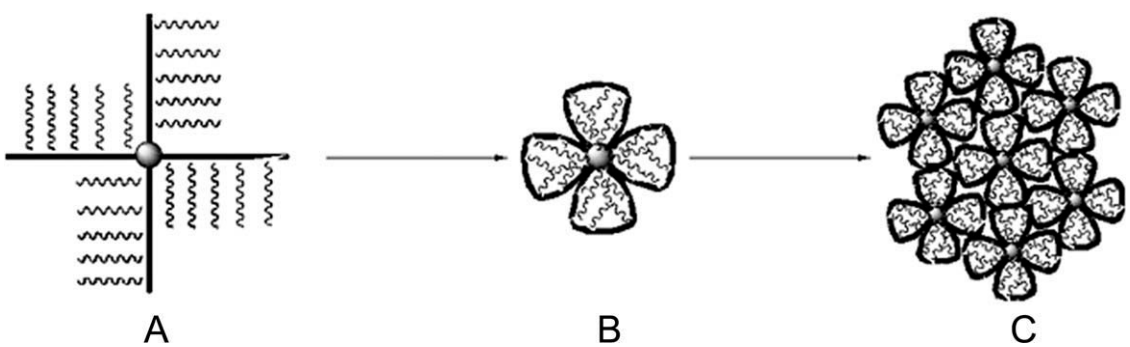

Figure 9 Schematic drawing illustrates the formation of star–comb block copolymer porphyrin-(PSt-*g*-PGMA)$_4$ micelles.

a hard PSt block. They can self-assemble in aqueous media to form polymeric nanospheres. The driving force for the nanospheres prepared from this copolymer probably involves strong repulsion between PSt blocks and PGMA blocks. Formation of polymeric nanospheres prepared from copolymer (PSt/PGMA = 75 : 63) in aqueous solution was judged from the bluish tinge of such a solution. The average hydrodynamic diameters for polymeric nanospheres were determined by DLS to be 197 nm with a dispersity of 0.271 (Fig. 6). AFM can be used to obtain measurements of the size and size distribution in the solid state, which eliminates perturbation caused by solvent swelling. By taking a cross section through the AFM height image, it was observed in Figure 7 that the well-defined, polymeric nanospheres were formed and had a diameter in the range of 110–130 nm. However, the hydrodynamic diameter from DLS (d_{DLS}) was much larger than d_{AFM}. The reason for this difference might be that the nanospheres were swollen in water during the DLS measurement, whereas AFM showed the diameter of nanospheres in the dry state.

The micelle formation was commonly monitored with fluorescence spectrum of pyrene probe. Polymer concentration dependence of I_{338}/I_{334} was shown in Figure 8. I_{338}/I_{334} increased from 0.56 to 1.3 with increasing polymer concentration **C** from 10^{-5} to 0.5 mg/mL, which indicated formation of micelles in aqueous solution with the star–comb polymer porphyrin-(PSt-*g*-PGMA)$_4$ (Fig. 9). The pyrene probe transferred from water phase into the micelle during the process of formation of micelles due to its hydrophobicity and the microenvironment of pyrene changed from high-polar water to less-polar micelles. The CMC value (0.00039 mg/mL) was determined from the intersection point of the tangents to the I_{338}/I_{334} vs. log *C* curve as demonstrated in Figure 8.

Also, we studied the influence of polymer concentration and temperature on the morphology. No significant change was observed. How is the formation of nanospheres? The mechanism was proposed like this. The polymer was dissolved in DMF. After the water was dropped in, the unimer was formed. However, the unimer was not stable due to the surface energy. To dissipate the surface energy and achieve a stable state, a lot of unimers were aggregated into multimers.

CONCLUSIONS

Amphiphilic star–comb polymer porphyrin-(PSt-*g*-PGMA)$_4$ has been successfully prepared from tetrafunctional star-shaped macroinitiator (Porphyrin-Br$_4$) via two steps of ATRP reaction. Polymers with a number-average molecular weight of 18,000 g/mol and low-dispersity index (M_w/M_n, 1.34) were obtained. The structure of the polymer was investigated by NMR, UV–vis, IR, and GPC measurement. The amphiphilic star–comb polymer porphyrin-(PSt-*g*-PGMA)$_4$ can self-assemble into polymeric nanospheres in aqueous solution. Porphyrin-(PSt-*g*-PGMA)$_4$ nanospheres had a diameter in the range of 110–130 nm by the measurement of AFM. Also, the mechanism of self-assembly was explained in detail. Simple and convenient synthesis method opened a new route to synthesize comb–star copolymers, which make it useful for the development of complex polymer synthesis.

References

1. Cammidge, A. N.; Lifsey, K. M. Tetrahedron Lett 2000, 41, 6655.
2. Feng, X.; Senge, M. O. Tetrahedron 2000, 56, 587.
3. Sun, E. J.; Cheng, X.; Wang, D.; Tang, X.; Yu, S.; Shi, T. Solid State Sci 2007, 9, 1061.
4. Li, X.; Zheng, Z.; Han, M.; Chen, Z.; Zou, G. J. Phys Chem B 2007, 111, 4342.
5. Zhang, H.; Ma, Y.; Lu, Z.; Gu, Z. Colloids Surf A 2005, 257–258, 291.
6. Hayval, M.; Gunduz, H.; Gunduz, N.; Kılıc, Z.; Hokelekb, T. J Mol Struct 2000, 525, 215.
7. Ohgo, Y.; Hoshino, A.; Okamura, T.; Uekusa, H.; Hashizume, D.; Ikezaki, A.; Nakamura, M. Inorg Chem 2007, 46, 8193.
8. Luca, G. D.; Pollicino, G.; Romeo, A.; Scolaro, L. M. Chem Mater 2006, 18, 2005.
9. Imahori, H.; Hayashi, S.; Hayashi, H.; Oguro, A.; Eu, S.; Umeyama, T.; Matano, Y. J Phys Chem C 2009, 113, 18406.
10. Schaefgen, J. R.; Flory, P. J. J Am Chem Soc 1948, 70, 2709.
11. Sanda, F.; Hitomi, M.; Endo, T. Macromolecules 2001, 34, 5364.
12. Calucci, L.; Forte, C.; Buwalda, S. J.; Dijkstra, P. J.; Feijen, J. Langmuir 2010, 26, 12890.
13. Saito, N.; Liu, C.; Lodge, T. P.; Hillmyer, M. A. ACS Nano 2010, 4, 1907.
14. Lanson, D.; Ariura, F.; Schappacher, M.; Borsali, R.; Deffieux, A. Macromolecules 2009, 42, 3942.
15. Kim, B. G.; Chung, J. S.; Sohn, E. H.; Kwak, S. Y.; Lee, J. C. Macromolecules 2009, 42, 3333.
16. Lanson, D.; Schappacher, M.; Borsali, R.; Deffieux, A. Macromolecules 2007, 40, 9503.
17. Zamurovic, M.; Christodoulou, S.; Vazaios, A.; Iatrou, E.; Pitsikalis, M.; Hadjichristidis, N. Macromolecules 2007, 40, 5835.
18. Pensec, S.; Nouvel, N.; Guilleman, A.; Creton, C.; Bou, F.; Bouteiller, L. Macromolecules 2010, 43, 2529.
19. Zhang, H.; Li, Y.; Zhang, C.; Li, Z.; Li, X.; Wang, Y. Macromolecules 2009, 42, 5073.
20. Jin, R. H. Adv Mater 2002, 14, 889.
21. Hecht, S.; Ihre, H.; Frechet, J. M. J. J Am Chem Soc 1999, 121, 9239.
22. Hecht, S.; Vladimirov, N.; Fréchet, J. M. J. J Am Chem Soc 2001, 123, 18.
23. Dai, X. H.; Dong, C. M.; Fa, H. B.; Yan, D.; Wei, Y. Biomacromolecules 2006, 7, 3527.
24. Li, B.; Xu, X.; Sun, M.; Fu, Y.; Yu, G.; Liu, Y.; Bo, Z. Macromolecules 2006, 39, 456.
25. Dichtel, W. R.; Baek, K. Y.; Fréchet, J. M. J.; Rietveld, I. B.; Vinagradov, S. A. J Polym Sci Part A: Polym Chem 2006, 44, 4939.
26. Celik, A.; Kemikli, N.; Ozturk, R.; Muftuoglu, A. E.; Yilmaz, F. React Funct Polym 2009, 69, 705.

27. Beil, J. B.; Zimmerman, S. C. Macromolecules 2004, 37, 778.
28. Yusa, S.; Endo, T.; Ito, M. J Polym Sci Part A: Polym Chem 2009, 47, 6827.
29. Boyer, C.; Stenzel, M. H.; Davis, T. P. J Polym Sci Part A: Polym Chem 2011, 49, 551.
30. High, L. R. H.; Holder, S. J.; Penfold, H. V. Macromolecules 2007, 40, 7157.
31. Dichtel, W. R.; Baek, K. Y.; Frechet, J. M. J.; Rietveld, I. B.; Vinogradov, S. A. J Polym Sci Part A: Polym Chem 2006, 44, 4939.
32. Matyjaszewski, K.; Xia, J. Chem Rev 2001, 101, 2921.
33. Liu, S. S.; Sen, A. Macromolecules 2001, 34, 1529.
34. Liu, S. S.; Sen, A. Macromolecules 2000, 33, 5106.
35. Adler, A. D.; Sklar, L.; Longo, F. R. J Heterocycl Chem 1968, 5, 669.
36. Schn, F.; Hartenstein, M.; Mller, A. H. E. Macromolecules 2001, 34, 5394.
37. Jakubowski, W.; Kirci-Denizli, B.; Gil, R. R.; Matyjaszewski, K. Macromol Chem Phys 2008, 209, 32.